High Optical Properties and Rectifying Behavior of ZnO (Nano and Microstructures)/Si Heterostructures

Ramin Yousefi, Muhamad. Rasat. Muhamad

Abstract—We investigated a modified thermal evaporation method in the growth process of ZnO nanowires. ZnO nanowires were fabricated on p-type silicon substrates without using a metal catalyst. A simple horizontal double-tube system along with chemical vapor diffusion of the precursor was used to grow the ZnO nanowires. The substrates were placed in different temperature zones, and ZnO nanowires with different diameters were obtained for the different substrate temperatures. In addition to the nanowires, ZnO microdiscs with different diameters were obtained on another substrate, which was placed at a lower temperature than the other substrates. The optical properties and crystalline quality of the ZnO nanowires and microdiscs were characterized by room temperature photoluminescence (PL) and Raman spectrometers. The PL and Raman studies demonstrated that the ZnO nanowires and microdiscs grown using such set-up had good crystallinity with excellent optical properties. Rectifying behavior of ZnO/Si heterostructures was characterized by a simple DC circuit.

Keywords—ZnO nano and microstructures, Photoluminescence, Raman, Rectifying behavior.

I. INTRODUCTION

ZNO is an important wide-band-gap semiconductor with a direct band-gap of 3.37 eV and a high exciton binding energy of 60 meV, which is greater than the thermal energy at room temperature. ZnO is a promising material for ultraviolet nano-optoelectronic devices and lasers operating at room temperature [1]. Recently, different methods have been applied to produce one-dimensional ZnO nanostructures such as pulsed laser deposition (PLD) [2-3], metal-organic chemical vapor deposition (MOCVD) [4-5], molecular beam epitaxy (MBE) [6], and solution processes [7]. Additionally, the use of metal catalysts such as Cu [8], Sn [9], NiO [10], and Au [1] and expensive substrates such as GaN [11], AlN [12], and sapphire [13] is very common for the growth of vertically aligned ZnO nanowires. PLD, MOCVD, and MBE require a complex and an expensive vacuum system. Furthermore, the use of a catalyst affects the optical and electrical properties; therefore, if catalysts are used to synthesize nanowires, they should be removed during the fabrication of the devices. Thus, the production of nanowires with the necessary properties for application in devices using an inexpensive method is one of the greatest challenges in this area. In addition, GaN, AlN, and sapphire are much more expensive than silicon, so their commercial potential has been limited. Of the various methods available for synthesizing nanowires, thermal evaporation methods and silicon substrates for the growth of 1D ZnO nanostructure present a particularly cost-effective and high-quality equilibrium process. It is also known that silicon plays a very important role in current opto-electronic technology,

due to its low cost. However, it is not generally preferred for the growth of ZnO nanostructures, due to the large lattice and thermal expansion coefficient mismatch between silicon and ZnO. Therefore, the exploration of simple, inexpensive, and catalyst-free methods for synthesizing high-quality vertically aligned ZnO nanowires grown on silicon substrates have remained as a great challenge.. In this work, we report well-aligned ZnO nanowires with different sizes as well as microdiscs grown on p-type Si (111) substrates by a modified thermal evaporation method, without using any metal catalysts, additives, complex procedures, or buffer layers. Our set-up is modified by using a double-tube system, in which the interior tube is a one-ended tube. Such a system makes the vapor environment regionally balanced and highly saturated, which is a key factor in the vertical growth of ZnO nanowires arrays. Different sizes of nanowires and morphologies are obtained by using substrates that are placed at different positions. The characterization shows that the optical and electrical properties of the resultant products are also improved by the use of this method.

II. EXPERIMENTAL DETAILS

ZnO nanowires and microdiscs were deposited in a horizontal double-tube system. First, p-type Si (111) substrates were ultrasonically cleaned using ethanol and de-ionized water, and they were then lightly etched using HF (43%) mixed with de-ionized water (1:10) for about 10 minutes to remove the native oxide layer. The double-tube system contains a quartz tube vacuum chamber 100 cm in length and 5 cm in diameter. A smaller one-ended quartz tube, 50 cm in length and 2 cm in diameter, which contained the precursor materials and substrate, was placed within the vacuum chamber. A mixture of zinc oxide powder (99.99%) and commercial graphite powder at a 1:1 weight ratio was used as the precursor material of ZnO. The precursor material of ZnO was placed at the closed end of the smaller quartz tube. Silicon substrates were located downstream from the source material. The source material was heated up to 950 °C, while the substrates were placed at 650, 600, and 550 °C and were kept at these temperatures for 1h. High-purity N_2 gas was fed at about 100 sccm into the furnace tube at one end, while the other end was connected to a rotary pump. A vacuum of 6 Torr was maintained inside the furnace tube during the deposition of the nanostructures. The crystal structure and morphology of the products were investigated by field emission scanning electron microscope (FESEM, Quanta 200F) and X-ray diffractometer (XRD, Siemens D5000).

Room temperature photoluminescence (PL) and Raman (Jobin Yvon Horiba HR 800 UV) measurements were employed to study the optical properties and crystallinity of the products using a He-Cd laser with a wavelength of 325 nm and an Ar ion laser with an emission wavelength of 514.5 nm for PL and Raman measurements, respectively.

III. RESULTS AND DISCUSSION

Figs 1(a_1)-(c_1) and 1(a_2)-(c_2) show low- and high-magnification FESEM images of the ZnO nanostructures, respectively, which were grown on various substrates.
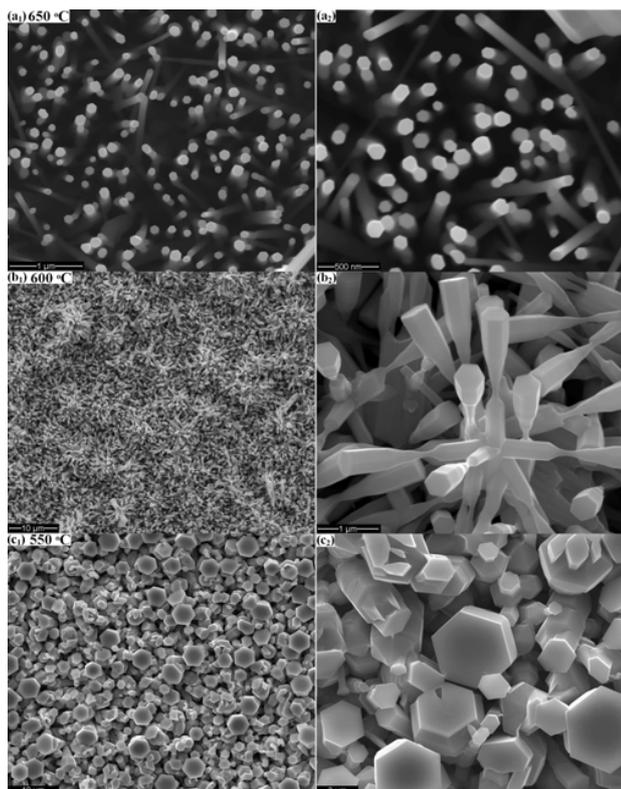
Fig. 1 (a_1) and (a_2): Low- and high-magnification FESEM images of ZnO nanowires grown at 650 °C, respectively. (b_1) and (b_2): Low- and high-magnification FESEM images of ZnO nanowires grown at 600 °C, respectively. (c_1) and (c_2): Low- and high-magnification FESEM images of ZnO microdiscs grown at 550 °C, respectively.

It is observed, thin nanowires grown (d ≈ 90 nm) at ~ 650 °C (a), thick nanowires grown (d ≈ 300 nm) at ~ 600 °C (b), and a mixture of microdiscs with a wide distribution of diameters grown (800 nm ≤ d ≤ 4 μm) at ~ 550 °C (c). It can be seen that, the formation of various ZnO products is only mixed for the sample that was placed the furthest from the source material. Nanostructures with different sizes were obtained in the different regions of the tube because the supersaturation of ZnO vapor differs in these zones. The supersaturation is one of the key factors in deforming the morphology of the nanostructures in the thermal evaporation method [14]. In addition, under high magnification as shown in Fig. 1(a_2)-(c_2), these nano and microstructures appear to have a perfect hexagonal geometry. The c-axis of ZnO is known to be perpendicular to its hexagonal cross section; therefore, the orientation of the nanowires and microdiscs growth is preferentially along the c-axis direction ([0001]). Additionally, because no catalyst was used in the growth of the ZnO nanowires or microdiscs in this study, the vapor-liquid-solid (VLS) mechanism cannot be responsible for their growth. The absence of detectable catalyst particles at the ZnO nanowire tips supports this statement.

Based on these results, the growth mechanism of ZnO nanowires and microdiscs can be tentatively proposed in this set-up. It is known that diffusion will occur even if the total pressure is uniform, as long as there is a spatial difference in the chemical potential, which is normally represented by differences in concentration or partial pressure, of the compounds of a gas mixture [16]. The fundamental equation used to describe one-dimensional diffusion of a gas is Fick's first law. According to Fick's law, the diffusion flux is:

$$J= -D(dN/dx) \tag{1}$$

where J is the net flux of vapors (per unit area per unit time), D is the diffusion constant, and (dN/dx) is the concentration gradients of the vapors along the propagation direction (x) [17]. This means that the diffusion will always propagate toward the region with a lower concentration. Based on these reasons, ZnO vapors can propagate toward the substrate in our configuration. Mensah *et al.* [18] used a similar method to grow ZnO nanostructures on silicon substrates coated with Au by controlled vapor concentration gradients. They suggested that controlled concentration gradients of not only ZnO vapors but also Au vapors could cause selective growth of the pure ZnO nanostructure. On the other hand, in our configuration only ZnO vapors are responsible for selective growth of pure ZnO nanostructures. In addition, the diffusion process of ZnO vapors could be affected by Au vapors along the tube furnace; therefore, Mensah *et al.* [18] obtained a mixture of different morphologies in all of their samples. In our set-up, ZnO nanostructures were grown on catalyst-free substrates, so, except for the furthest sample, the samples contain a uniform distribution of ZnO nanowires. One question here is: why does sample (c) contain a variety of microdiscs sizes, while the other samples contain nanowires of approximately uniform size? The final sample is close to the one-ended tube edge, where a small amount of N_2 gas can enter into the one-ended tube (Fig. 2). The diffusion of the N_2 gas cannot occur much further along the tube due to the tube temperature increase from edge to the end that is placed in the center of furnace (green arrows in Fig. 2). Therefore, when ZnO vapors reach the furthest sample, they are affected by the N_2 gas. This collision between two gases disturbs flow uniformity of the ZnO vapors in this region. Consequently, the non-uniform ZnO vapors found at this sample causes the growth of ZnO

microdiscs with polydispersity. On the other hand, N_2 gas cannot further affect the ZnO vapors at sample (b) or (a), which are placed at higher temperatures (Fig. 2).
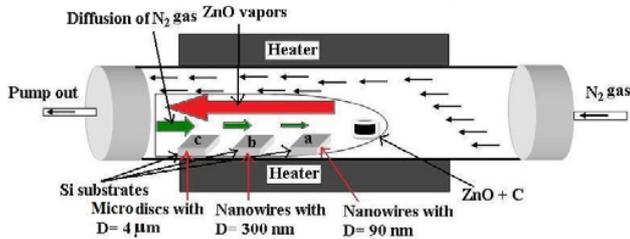
Fig. 2 Green arrows show the diffusion of N_2 gas along the one-ended tube from the edge of the tube. In addition, the size of the green arrows shows that the diffusion of the N_2 gas along the tube decreases from the edge to the end of the tube that is placed at the center of furnace.

Therefore, due to the flow uniformity of the ZnO vapors at these regions, nanowires grow on substrates (a) and (b) with monodispersity. The other question here is: why does the diameter of the nanowires increase from sample (a) to (c)? This question has been answered by Li *et al.* [19]. They suggested that the size of the nucleating nanocrystals, which form at certain locations to relieve strain, increases with decreasing substrate temperature. At high substrate temperatures, rapid nanowire growth begins immediately after nanocrystal formation, freezing in the minimum nanocrystal diameter. For decreasing substrate temperature, the nanocrystals have more opportunity to grow laterally in order to distribute strain relief before vertical nanowire or microdiscs growth begins.

Fig 3 shows XRD patterns for the ZnO nanowires and microdiscs that were grown at the different temperatures regions: (a) 650 °C, (b) 600 °C, and (c) 550 °C. The XRD patterns in Fig. 3 agree with the standard card of bulk ZnO with a hexagonal structure (JCPDS No. 800075). No peaks from Zn or other impurities are visible. The dominant (002) peak for samples (a) and (c) indicates that the c-axis of the ZnO nanowires and microdiscs in these samples is perpendicular on the substrate.

Fig 4 shows the room temperature PL spectra of the ZnO nanowires and microdiscs that were grown at different temperatures: (a) 650 °C, (b) 600 °C, and (c) 550 °C. All of the PL spectra show a strong peak in the ultraviolet (UV) region at 381 nm and negligible green emission (deep-level emission (DLE)) peaks at 520 nm in the visible region. UV emission is also called the near-band-edge (NBE) emission, due to the recombination of free excitons through an exciton-exciton collision process. It has been suggested that DLE corresponds to the singly ionized oxygen vacancy in ZnO and results from the recombination of a photo-generated hole with the singly ionized charge state of this defect [20]. Therefore, Fig. 4 shows that the ZnO nanowires and microdiscs have very low concentrations of oxygen vacancies. In fact, the concentrations of the Zn and O vapors can be increased in this set-up; therefore, the oxygen vacancy can be decreased in

such set-up. Ratio of the UV to DLE peak is one of the main factors that uses for comparing optical properties between samples. The UV/DLE ratio peak increases from sample (a) to (c). Therefore, the crystallinity of the microdiscs is higher than that of the nanowires. According to FESEM results, the average diameter of the ZnO nanostructures increases from sample (a) to (c). In our previous work [21], we showed a relationship between the aspect ratio (L/D) of ZnO nanowires and PL emissions. The UV emission was more intense in nanowires with a small aspect ratio, while the DLE emission dominated in nanowires with a large aspect ratio.
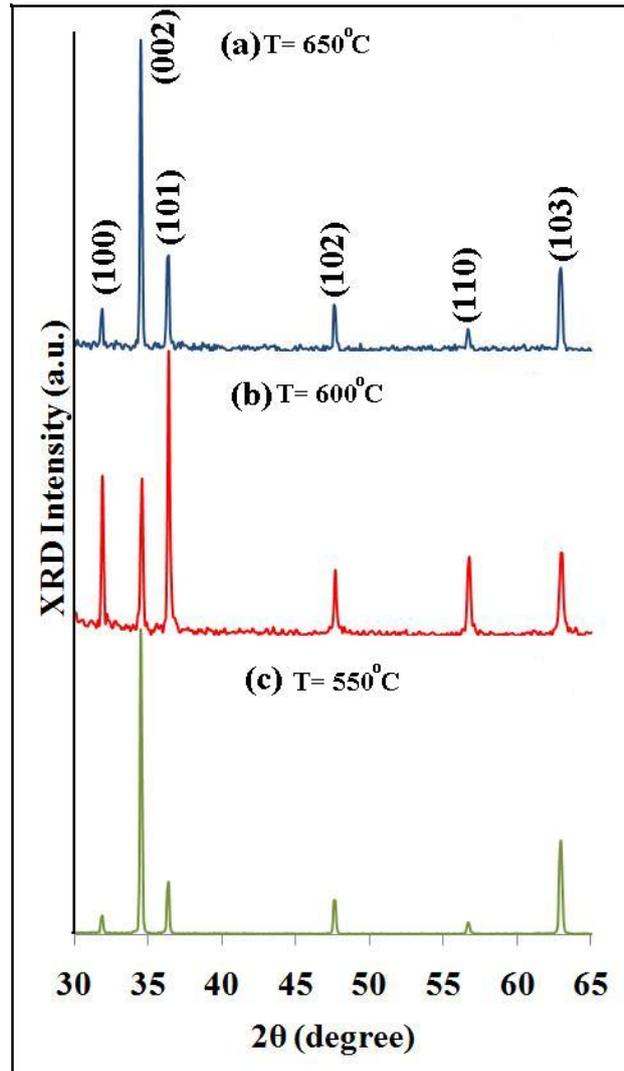
Fig. 3 XRD patterns for the ZnO nanowires and microdiscs that were grown in different temperatures regions: (a) 650 °C, (b) 600 °C, and (c) 550 °C.

We suggested that surface effects most likely contribute significantly to the DLE emission. As the dimensions of the ZnO nanostructures decrease the number of surface atoms will be greater than the number of atoms in the bulk material, and surface state densities and surface defects will be dominant.

DLE emission is usually related to such various defects. The results obtained here are in agreement with our previous results.
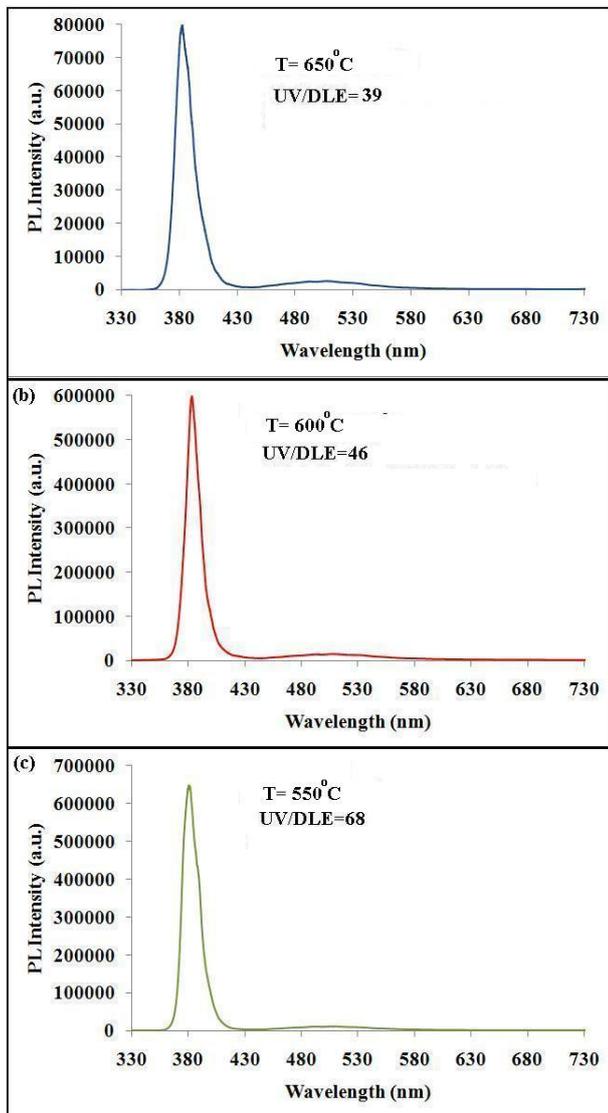
Fig. 4 Room temperature PL spectra of the ZnO nanowires and microdiscs that were grown at different temperatures: (a) 650 °C, (b) 600 °C, and (c) 550 °C.

Raman spectroscopy is an effective technique for estimating the crystallinity of materials. According to group theory, single crystalline ZnO belongs to the C_4^{6V} space group having two formula units per primitive cell and eight sets of optical phonon modes at the Γ point of the Brillouin zone, classified as $A_1 + E_1 + 2E_2$ modes (Raman active), $2B_1$ modes (Raman silent), and $A_1 + E_1$ modes (infrared active). The E_1 mode is a polar mode and is split into transverse optical (TO) and longitudinal optical (LO) branches. Fig 5 shows the Raman spectra of the ZnO nanowires and microdiscs that were grown at different temperatures: (a) 650 °C, (b) 600 °C, and (c) 550

°C. As shown in Fig. 5, the Raman spectra of all nano and microstructures show an E_{2H}-E_{1L} peak at 329 cm^{-1} and an A_{1T} peak at 379 cm^{-1}. In addition the spectra exhibit a sharp, strong, and dominant peak at 437.8-439 cm^{-1}, corresponding to the E_2(high) mode of the Raman active mode, a characteristic peak for the wurtzite hexagonal phase of ZnO [23].
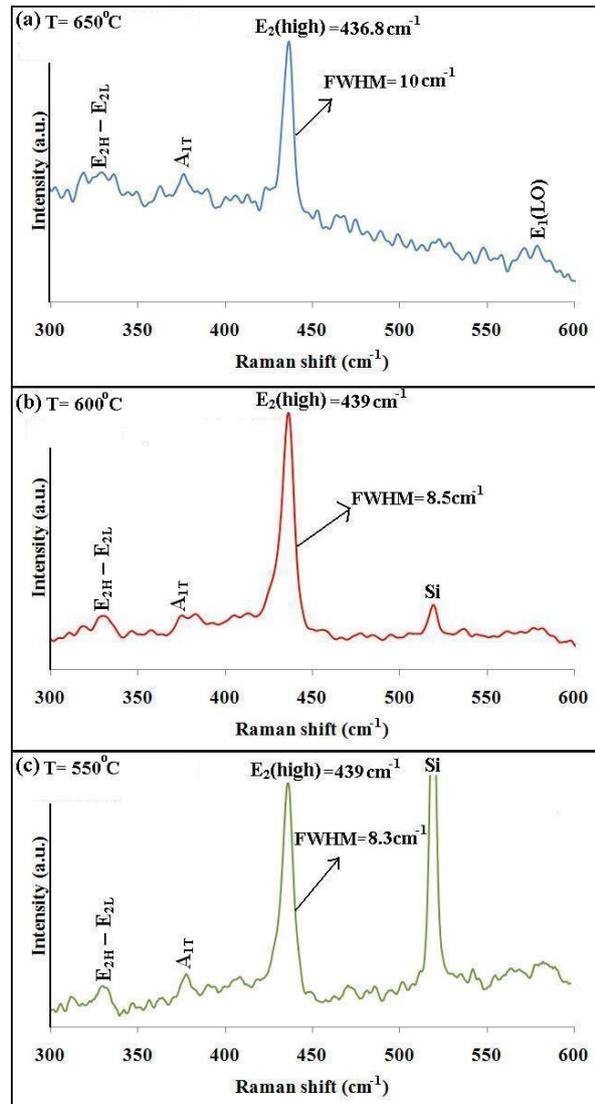
Fig. 5 Raman spectra of the ZnO nanowires and microdiscs that were grown at different temperatures: (a) 650 °C, (b) 600 °C, and (c) 550 °C.

Furthermore, as shown in Fig. 5, the FWHM of the E_2(high) peak decreased from sample (a) to sample (c). Therefore, these results and the PL results show that the crystallinity of the microdiscs is higher than that of the nanowires. Fig 5 (a) shows an additional peak at 576 cm^{-1} that corresponds to the E_1(LO) mode for nanowires grown at 650 °C. The E_1(LO) mode is associated with impurities and formation of defects such as oxygen vacancies [23]. Therefore, the appearance of

the $E_1(LO)$ mode for sample (a), indicates a lower crystalline quality and a higher oxygen vacancy for the ZnO nanowires grown on the substrates in a 650 °C environment, in comparison with the other nanostructures.

I –V characteristics of the ZnO nanowires grown at 650 °C and ZnO microdiscs grown at 550 °C are performed by large area Ag contact. The I –V curves exhibit a rectifying behavior with a rectification ratio (I_F/I_R) of 31 for the nanowires and 42 for the microdiscs at 400 mV. Bigger rectification ratio of the microdiscs than the nanowires is due to bigger top surface of the microdiscs; therefore, contact of these discs is better than the nanowires. In addition, crystalline quality of the nanowires decreases and crystal defects increases due to increase of the surface to volume ratio in such nanostructures. The turn-on voltage is observed to be around 100 mV for the both samples. The results indicate that the ZnO nanowires and microdiscs that deposited on p-type Si substrates can be used as a rectifying diode.
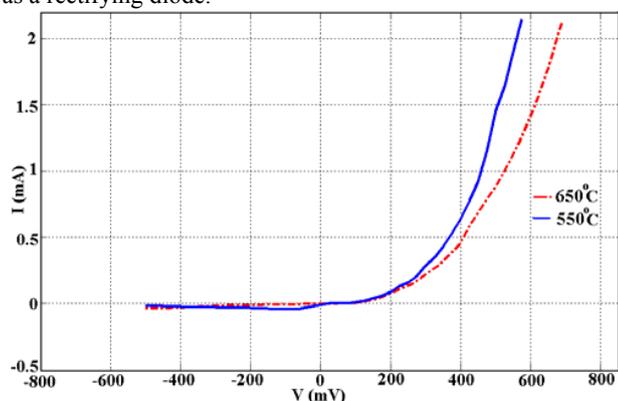
Fig. 6. I-V curve of ZnO nanowires and microdiscs grown at 650 and 550 °C, respectively.

IV. CONCLUSION

ZnO nanowires and microdiscs were successfully deposited on p-type Si(111) substrates at different temperatures using a modified thermal evaporation method, without the use of a metal catalyst. A one-ended quartz tube was used as a tool to modify the thermal evaporation process and caused the concentrations of Zn and O to increase in the tube. The diameter of the ZnO nanowires increased with increasing distance between the samples and the source materials. In contrast to the ZnO nanowires, the sample that contained microdiscs showed a distribution of microdiscs with polydispersity. The PL and Raman measurements exhibited a high optical efficiency and crystallinity for the ZnO nanowires and microdiscs. In addition, these characterizations showed that the crystallinity of the nanowires decreased with decreasing nanowires diameter. ZnO (nano and microstructures)/Si(111) showed a high rectifying behavior.

REFERENCES

[1] M.H. Huang, S. Mao, H. Yan, Y. Wu, H. Kind, E. Weber, R. Russo and P. Yang, Science 292 (2002) 1897.
[2] T. Premkumar, P. Manoravi, B.K. Panigrahi, K. Baskar, Appl. Surf. Sci 255 (2009) 6819.
[3] Y. Ma, C.P. Wong, X.T. Zeng, T. Yu, Y. Zhu, Z.X. Shen, J. Phys. D: Appl. Phys. 42 (2009) 065417.
[4] D.J.Park, D.C. Kim, J.Y. Lee1, H.K. Cho, Nanotechnology 17 (2006) 5238.
[5] Y.J. Tak, Y.H. Ryu, K. Yong, Nanotechnology 16 (2005) 1712.
[6] L.C. Tien, D.P. Norton, S.J. Pearton , H.T. Wang, F. Ren, Appl. Surf. Sci 253 (2007) 4620.
[7] Y. Liu, Z. H. Kang, Z. H. Chen, I. Shafiq, J. A. Zapien, I. Bello,W. J. Zhang, S. T. Lee, Crystal Growth & Design, 9 (2009) 3223.
[8] S.Y. Li, C.Y. Lee and T.Y. Tseng, J. Cryst.Growth 247 (2003) 357.
[9] P.X. Gao, Y. Ding and Z.L. Wang, Nano Letters 3 (2003) 1315.
[10] S.C. Lyu, Y. Zhang, C.J. Lee, H. Ruh and H.J. Lee, Chem. Mater. 15 (2003) 3294.
[11] E. Lai, W. Kim, P. Yang, Nano Res 1 (2008) 123
[12] L. Wang, Y. Pu, Y.F. Chen, C.L. Mo, W.Q. Fang, C.B. Xiong, J.N. Dai, F.Y. Jiang, J. Cryst.Growth 284 (2005) 459.
[13] J.H. He, J.H. Hsu, C.W. Wang, H.N. Lin, L.J. Chen, Z.L. Wang, J. Phys. Chem. B, 110 (2006), 50
[14] C. Ye, X. Fang, Y. Hao, X. Teng and L. Zhang, J. Phys. Chem. B 109 (2005) 19758.
[15] Z.L. Wang, J. Phys.: Condens. Matter 16 (2004) R829.
[16] C. Kittel, Thermal Physics; First ed; John Wily & Sons, Inc. New York 1969.
[17] C. Kittel, Introduction to Solid State Physics; 6th ed; Wiley, New York 1986.
[18] S.L. Mensah, V.K. Kayastha, Y.K. Yap, J. Phys. Chem. C 111 (2007) 16092.
[19] J. Li, Q. Zhang, H. Peng, H.O. Everitt, L. Qin, J. Liu, J. Phys. Chem. C 113 (2009) 3950.
[20] K. Vanheusden, W.L. Warren, C.H. Seager, D.R. Tallant, J.A. Voigt and B.E. Gnade, J. Appl. Phys, 79 (1996) 7983.
[21] R. Yousefi, B. Kamaluddin, J. Alloy Compd. 479 (2009) L11.
[22] A. Umar, Y.B. Hahn, Appl. Phys. Lett. 88 (2006) 173120.
[23] A. Umar, S.H. Kim, Y.S. Lee, K.S. Nahm, Y.B. Hahn, J. Cryst. Growth 282 (2005) 131-36.